Cytoplasmic Chaperonin Containing TCP-1: Structural and Functional Characterization†

Ronald Melki,* Gérard Batelier, Stéphanie Soulié, and Robley C. Williams, Jr.‡

Laboratoire d'Enzymologie et Biochimie Structurales, Centre National de la Recherche Scientifique, 91198 Gif-sur-Yvette, France

Received November 15, 1996; Revised Manuscript Received March 12, 1997⊗

ABSTRACT: Actin and tubulin polypeptide chains acquire their native conformation in the presence of the cytoplasmic chaperonin containing TCP-1 (CCT, also called TRiC) and, in the case of α- and β-tubulin, additional protein cofactors. It has been previously demonstrated that nucleotide exchange and ATP hydrolysis act to switch CCT between conformations that interact either strongly or weakly with unfolded substrates [Melki, R., & Cowan, N.J. (1994) *Mol. Cell. Biol. 14*, 2895−2904]. The present study further documents the conformational changes and function of CCT. It is first shown, by the use of a range of labeled denatured substrate proteins and a radiolabeled total soluble HeLa cell extract, that CCT in the absence of nucleotides can bind any of a large number of proteins *in vitro* with high affinity. Second, by the use of denatured labeled β-actin and β-tubulin as model substrates for binding to CCT, we demonstrate that the CCT particle can contain two substrate protein chains simultaneously. Third, by electron microscopy, sedimentation velocity, and intrinsic fluorescence measurements, we document the conformational difference between CCT in its ATP- and ADP-bound forms, as well as the change that results from binding of substrate protein. A model summarizes substrate association with CCT and the role of the nucleotide in regulating the affinity of CCT for target proteins.

There is compelling evidence that many cellular proteins need to interact with a class of polypeptides known as molecular chaperones in order to acquire their native states [reviewed by Gething and Sambrook (1992) and Hartl (1996)]. The chaperones recognize and bind proteins in their non-native state and assist them to fold into their native conformation [reviewed by Gething and Sambrook (1992), Hartl *et al*. (1992), Morimoto *et al*. (1994), and Hartl (1996)]. They seem to act by stabilizing the conformations of folding intermediates, thereby preventing aggregation and directing the newly formed polypeptides toward correct folding, assembly, and translocation (Ellis & van der Vies, 1991; Hartl, 1996).

The chaperonins (Hemmingsen *et al*., 1988), a subgroup of the molecular chaperones, are ubiquitous multimeric cylindrical complexes [reviewed by Kubota *et al*. (1995) and Hartl (1996)]. They are exemplified by the well-known bacterial chaperonin GroEL (Georgopoulos *et al*., 1973). CCT,[1] a homolog of GroEL, is found in the cytosol of eukaryotic cells (Gao *et al*., 1992; Yaffe *et al*., 1992; Lewis *et al*., 1992; Frydman *et al*., 1992). Among the polypeptides whose folding it facilitates are actins and tubulins (Gao *et al*., 1992; Yaffe *et al*., 1992; Frydman *et al*., 1992; Melki *et al*., 1993). Unlike GroEL, which is a homooligomer, this chaperonin is composed of eight to nine different, but related, polypeptides (Lewis *et al*., 1992; Rommelaere *et al*., 1993; Kubota *et al*., 1994), one of which is TCP-1 (Willison *et al*., 1986). It is therefore referred to as the chaperonin-containing TCP-1 (CCT) (Kubota *et al*., 1995), as TCP-1 ring complex (TRiC) (Frydman *et al*., 1992), or as cytoplasmic chaperonin (Gao *et al*., 1992) because of its localization (Lewis *et al*., 1992).

GroEL seems to be involved in the facilitated folding of a very wide variety of *Escherichia coli* proteins (Horwich *et al*., 1993; Viitanen *et al*., 1992). In contrast, studies of CCT's substrate preferences in crude cellular extracts have led to the tentative conclusion that it is involved chiefly, or perhaps exclusively, in the folding of actin and tubulin (Gao *et al*., 1992, 1993; Yaffe *et al*., 1992; Sternlicht *et al*., 1993). Nevertheless, some reports have noted the binding of measurable amounts of several other proteins to CCT[2] (Frydman *et al*., 1992; Melki & Cowan, 1994; Hynes *et al*., 1996) and its involvement in folding a viral capsid protein (Lingappa *et al*., 1994). When firefly luciferase is presented to CCT as a purified protein, it is also bound and folded (Frydman *et al*., 1992). These results lead one to question whether the apparent narrow specificity of CCT may be an artifact resulting from the presence of high concentrations of actin and tubulin in cell extracts. To understand this problem, we have chosen several denatured labeled proteins and assayed their binding to CCT when they are added in a purified state. For comparison, we have examined the spectrum of proteins bound by CCT from crude extracts of HeLa cells.

† This work was supported by grants from the Centre National de la Recherche Scientifique, the Association pour la Recherche sur le Cancer, and the Ligue Nationale Française Contre le Cancer (to R.M.) and by Grant GM25638 of the U.S. National Institutes of Health and funds from the Vanderbilt University Research Council (to R.C.W.).

* Corresponding author. Phone: 33-1-69-82-35-03. Fax: 33-1-69-82-31-29. E-mail: melki@lebs.cnrs-gif.fr.

‡ Permanent address: Vanderbilt University, Department of Molecular Biology, Box 1820, Station B, Nashville, TN 37235. Phone: 1-615-322-2072. Fax: 1-615-343-6707. E-mail: williarc@ctrvax.vanderbilt.edu.

⊗ Abstract published in *Advance ACS Abstracts,* May 1, 1997.

[1] Abbreviations: ADF1, actin depolymerizing factor 1; CCT, chaperonin-containing TCP-1; DTT, dithiothreitol; EGTA, ethylene glycol bis(β-aminoethyl ether)-*N*,*N*,*N*′,*N*′-tetraacetic acid; folding buffer, 80 mM MES, pH 6.8, 1 mM EGTA, 1 mM $MgCl_2$, 1 mM ATP, 1 mM GTP, and 1 mM DTT; MES, 2-(*N*-morpholino)ethanesulfonic acid.

[2] Acetylcholinesterase polypeptide chains bind also to CCT *in vitro*, while profilin does not (N. Morel and R. Melki, unpublished observations).

S0006-2960(96)02830-9 CCC: $14.00

Results suggest that CCT may have broad recognition capabilities.

The mechanism of chaperonin-assisted folding is still something of a mystery. Folding is believed to take place within the central cavity of CCT while the substrate (hereafter called the *target protein*) is sequestered by the molecular chaperone. Both GroEL and CCT appear in the electron microscope as symmetrical double toroids, and each could have two apparently equivalent potential binding sites for target proteins (Saibil *et al*., 1993; Braig *et al*., 1993, 1994; Marco *et al*., 1994; Chen *et al*., 1994; Azem *et al*., 1994; Schmidt *et al*., 1994; Todd *et al*., 1994; Fenton *et al*., 1994; Hartl, 1994; Roseman *et al*., 1996). In the absence of nucleotide, GroEL particles have been observed in the electron microscope to bind two target proteins, one in each of the central cavities (Braig *et al*., 1993). Functionally, though, the binding of target protein to the GroEL/GroES complex appears to be negatively cooperative in the sense that the binding of a target protein at one end of the particle excludes binding of a second at the other end [reviewed by Hartl (1996)]. In the case of CCT, nothing is known about such cooperativity, not even whether one chaperonin particle can bind one substrate molecule or two (one at either end). To have a chance to measure the maximum capacity of CCT for target proteins, it is essential to use CCT in its high-affinity state: in the absence of ATP. This tactic has been adopted in the past to investigate the capacity of myosin for binding actin (Eisenberg & Moos, 1968; Eisenberg *et al*., 1968; Valentin-Ranc *et al*., 1991). We investigated this issue by purifying β-actin− and β-tubulin−CCT binary complexes in the absence of ATP and then deducing the ratio of the number of radiolabeled denatured β-actins or β-tubulins bound per CCT.

Like the bacterial chaperonin GroEL, CCT adopts different conformations in the presence of ADP or ATP. The nature of the bound nucleotide also modulates CCT's affinity for target proteins (Melki & Cowan, 1994). In the long run it will be useful to understand the relationship between the structural changes and the binding-and-release functions of the chaperonins. In the case of CCT, the ADP- and ATP-mediated conformations are easily visible in the electron microscope because CCT becomes adsorbed to the surface of an electron microscope grid largely in an end-on fashion (*i.e*., rotational axis perpendicular to the surface) either when nucleotide is absent or when ADP is present, while many particles apparently lying on their sides appear in the presence of ATP (Gao *et al*., 1992; Marco *et al*., 1994). The ATP-bearing conformation of CCT appears more conical at its ends than does the ADP-form, when both are seen in "side-view" (Marco *et al*., 1994). Beyond these electron microscopic results, though, little is known about the two forms: about the kinetics of interconversion between them, about the relative nucleotide affinities that drive the interconversion, or indeed whether the two forms differ greatly or only marginally in their volume or shape. By combining electron microscopy, sedimentation velocity, sedimentation equilibrium, and intrinsic fluorescence measurements, this study shows the conformational changes to be relatively large and slow.

EXPERIMENTAL PROCEDURES

Materials. MES buffer was purchased from Calbiochem. ATP−agarose (ATP coupled through C8), ethylene glycol bis(β-aminoethyl ether)-*N*,*N*,*N*′,*N*′-tetraacetic acid (EGTA) and sodium dodecyl sulfate (SDS) were from Sigma. Adenosine 5′-triphosphate (ATP), adenosine 5′-diphosphate (ADP), guanosine 5′-triphosphate (GTP), and 1,4-dithiothreitol (DTT) were from Boehringer. $Al(NO_3)_3 \cdot 9H_2O$ ("Gold Label" grade) came from Aldrich. [^{35}S]-L-Methionine came from Amersham. All other chemicals were analytical grade.

Purification of the Chaperonin-Containing TCP-1. Rabbits were made anemic by injection of acetylphenylhydrazide, and rabbit reticulocyte lysate was prepared as described (Darnbrough *et al*., 1973). CCT was purified from rabbit reticulocyte lysate by the chromatographic method described by Gao *et al*. (1992). Fractions containing CCT that emerge from the ATP−agarose were pooled and concentrated by ultrafiltration (Centricon 30, Amicon Inc., Beverly, MA), and approximately 250 μL was applied to a Superose 6 column (HR 10/30, Pharmacia) equilibrated in 80 mM MES, pH 6.8, 1 mM EGTA, 1 mM $MgCl_2$, and 1 mM DTT. Contaminating Hsp70 and Hsc70 were depleted from this preparation by pooling the CCT-containing fractions that emerge from the Superose 6 column and applying them to a 1 mL column of a monoclonal antibody directed against Hsp70 and Hsc70 (N27F3-4, StressGen Biotechnologies Corp., Victoria, British Columbia, Canada), immobilized on protein-A−Sepharose Fast Flow column (Pharmacia). Of the material emerging from this column, 95% corresponded to the polypeptide chains that constitute CCT, as judged from running this material on a 10% SDS−polyacrylamide gel.

Preparation of Labeled Target Proteins and in Vitro Folding Reactions. ^{35}S-labeled unfolded β-tubulin and β-actin target proteins were generated by expression of appropriate clones in *E. coli* and purified as described by Gao *et al*. (1992, 1993). Denatured ^{35}S-labeled actin-RPV, TCP-1α, γ-tubulin, CAP-binding protein, p21^{ras}, and cyclin B were obtained as recombinant proteins as described in Melki *et al*. (1993) and in Melki and Cowan (1994). *In vitro* folding assays and analysis of the reaction products on nondenaturing polyacrylamide gels were performed in folding buffer, which consists of 80 mM MES, pH 6.8, 1 mM EGTA, 1 mM $MgCl_2$, 1 mM DTT, 1 mM ATP, and 1 mM GTP, as described previously (Gao *et al*., 1993). Following staining in Coomassie blue and destaining, the gels were fluorographed by the use of Amplify (Amersham) and dried. The yield of various products identified on the gel was quantified by the use of a phosphorimager.

Preparation of Total Soluble HeLa Cell Proteins. HeLa cells were labeled at 75% confluence by incubation for 4 h in Dulbecco's modified Eagle's medium lacking methionine and containing ^{35}S-labeled methionine (0.2 mCi/mL). Cells were harvested and homogenized in a glass Dounce homogenizer in 0.1 M MES, pH 6.8, 1 mM $MgCl_2$, 1 mM EGTA, 1 mM DTT, and 0.05% Triton X-100. The suspension was clarified by centrifugation at 100000*g* for 15 min at 4 °C. The proteins in the supernatant were denatured by addition of 7.5 M urea. The specific radioactivity of the final product was 7×10^7 cpm/mg.

Preparation of CCT−Target Protein Binary Complex. Complexes between CCT and β-actin or β-tubulin were prepared by incubating in nucleotide-free folding buffer, for 30 min at 25 °C, a mixture of Superose-6-purified CCT (2.5−6 μM) and a 10-fold molar excess of the target protein in the absence of ATP. The β-actin− or β-tubulin−CCT complexes were separated from unbound target proteins by gel filtration over a Superose 6 column. The fractions containing the binary complex were applied to a 1 mL column of anti-Hsp70/Hsc70 antibodies immobilized on protein-A− Sepharose (Pharmacia) in order to trap small amounts of Hsp70 or Hsc70 that contaminate this material.

Sedimentation Velocity and Molecular Mass Determination. Sedimentation velocity experiments were carried out with a Beckman Optima XLA ultracentrifuge equipped with an AN 60Ti four-hole rotor and cells with two-channel 12 mm path length centerpieces. Measurements were made at 40 000 rpm and 20 °C. Data were analyzed to provide the apparent distributions of sedimentation coefficients by means of the program DCDT (Stafford, 1992). Equilibrium sedimentation was performed in the same instrument, but at 4 °C. Sample volumes of 100 μL were centrifuged at 3400 rpm, after overspeed at 5900 rpm for 45 min. Radial scans of absorbance at 278 nm were taken at 1 h intervals in order to monitor the attainment of equilibrium. Equilibrium was reached after 12 h of centrifugation. The data were analyzed to yield weight−average molecular masses at the midpoint of the liquid column by use of the programs XLAEQ and EQASSOC supplied by Beckman. The partial specific volume was calculated to be 0.738 $cm^3\ g^{-1}$, and the solvent density was 1.01 g/cm^3.

Electron Microscopy. Samples were prepared in 80 mM MES, pH 6.8, 1 mM EGTA, 1 mM $MgCl_2$, and 1 mM DTT containing either 250 μM ADP or 250 μM ATP or both 250 μM ATP and 5 mM NaF and 100 μM $Al(NO_3)_3$. The latter two components produce the AlF_4^- ion, an effective inhibitor of turnover at the ATP-hydrolysis sites (Bigay *et al*., 1985; Carlier *et al*., 1988; Combeau & Carlier, 1988). At different times after addition of ADP, of ATP alone, or of ATP + AlF_4^-, carbon-coated grids (200 mesh) were floated for 1 min on a drop of sample, washed with the same buffer, and stained with a drop of 1% uranyl acetate. The grids were examined with a Philips EM 410 electron microscope.

Fluorescence Measurements. The intrinsic fluorescence of CCT (0.4 mL samples of 0.5 μM CCT in 4 × 4 mm square-section cuvettes) in the presence of ADP or ATP (100 μM) was recorded at 20 °C in a Spex Fluorolog 2 spectrofluorometer. The excitation monochromator was set at 295 nm and the emission was recorded between 300 and 500 nm.

Generation of Polyclonal Antibodies against TCP-1α. TCP-1α, purified by SDS−gel electrophoresis from inclusion bodies in *E. coli*, was injected into rabbits together with Freund's adjuvant. Five booster injections were given at intervals of 2 weeks. Specificity of the antiserum was tested by the use of purified CCT. The antibody binds to only one band, corresponding to TCP-1α, among the five bands that constitute the typical pattern of purified CCT on SDS gels.

Additional Methods. Protein concentrations were determined by either the Lowry or the Bradford method. Molecular masses of 800 000, 50 000, and 42 000 were employed for the estimation of CCT, β-tubulin, and β-actin

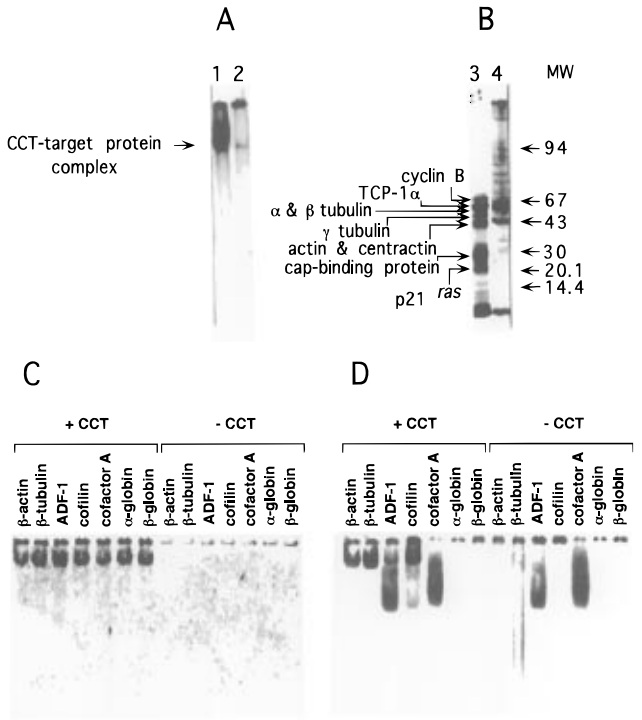

FIGURE 1: Spectrum of target protein recognition by the TCP-1-containing chaperonin. (A) Lane 1, a mixture of labeled, denatured target proteins (β-actin, α-, β-, and γ-tubulin, actin-RPV, cap-binding protein, cyclin B, $p21^{ras}$, and TCP-1α), each at the same specific radioactivity and concentration (20 pmol), was diluted 100-fold into CCT (5 pmol) in folding buffer containing no nucleotides. The reaction mixture was incubated 30 min at 30 °C, and the reaction products were separated on a 4% nondenaturing polyacrylamide gel and autoradiographed; lane 2, labeled, soluble HeLa cell proteins were denatured and presented to CCT as in lane 1. (B) Lanes 3 and 4, autoradiogram of target protein−CCT complexes isolated from lanes 1 and 2, respectively, of the nondenaturing gels shown in panel A, denatured and subjected to electrophoresis on 12% SDS−polyacrylamide gels. Arrowheads indicate the positions of the different target proteins and of the molecular weight markers. (C and D) Labeled, denatured β-actin, β-tubulin, *Arabidopsis thaliana* actin depolymerizing factor 1, human brain cofilin, cofactor A, and rabbit α- and β-globin were diluted from denaturant in the presence or absence of CCT (5 pmol) in folding buffer containing no nucleotide. The reactions were incubated under the same conditions as in panel A, and the products were analyzed on a 4% nondenaturing polyacrylamide gel. (C) Coomassie blue staining of the gel; (D) autoradiograph of the same gel.

molarities, respectively. SDS−polyacrylamide gel electrophoresis in 10% gels was performed by standard methods (Laemmli, 1970). Western blots were probed with the antibodies described above and developed with the enzyme-coupled luminescence technique (ECL, Amersham), according to the recommendation of the manufacturer.

RESULTS

Specificity of CCT

To investigate the question of the specificity of CCT, a mixture of denatured target proteins, each at the same specific radioactivity (β-actin, α-, β-, and γ-tubulin, actin RPV, cap-binding protein, cyclin B, $p21^{ras}$, and TCP-1α) was incubated with CCT. The binary complex was then isolated from a native gel by cutting out the appropriate band (Figure 1, lane 1), incubating the gel fragment in SDS sample buffer and subjecting it to electrophoresis on a 12% SDS−PAGE gel. Figure 1B, lane 3, shows that each of the proteins in the

artificial mixture binds efficiently to CCT.[3] A total labeled soluble HeLa cell extract was also diluted from denaturant into a nucleotide-free folding reaction mixture containing CCT and treated as above. In this experiment (native gel, lane 2, and SDS gel, lane 4), one sees that actin (apparent MW = 44 000) and tubulin (apparent MW = 55 000) are the most visible polypeptides that bind to CCT, but one can also clearly see that a large number of other proteins with molecular masses in the range 30000−120000 have bound to CCT. Because actins and tubulins are synthesized in greater amounts than other polypeptides (Spiegelman *et al*., 1977), their specific radioactivity in cellular extracts would be expected to be higher than that of other polypeptides. From these experiments, we conclude that CCT does not bind tubulins and actins exclusively. To the contrary, it binds a number of proteins.

Figure 1, panels C and D, shows results of a CCT-binding assay with another set of target proteins, investigated one at a time under identical conditions. ^{35}S-Labeled recombinant α- and β-globin (Gao *et al*., 1993), cofactor A (Melki *et al*., 1996), *Arabidopsis thaliana* ADF1, and human brain cofilin (Carlier *et al*., 1997) were presented individually to CCT, and the reaction products were analyzed on a nondenaturing polyacrylamide gel. *A. Thaliana* ADF1 and human brain cofilin were found to bind efficiently to CCT while α- and β-globin as well as cofactor A were not found to bind to CCT. We conclude from these experiments that CCT is not wholly promiscuous despite its capacity for binding a wide range of target proteins.

Saturation

To establish whether binding of β-actin and β-tubulin to CCT can be saturated, increasing amounts of the labeled denatured proteins were added to a constant amount of CCT by rapid 100-fold dilution of the denatured polypeptide in the absence of nucleotide, *i.e*., under conditions where CCT binds target proteins with high affinity. The amounts of bound polypeptide were quantitated following separation of the reaction products on a nondenaturing polyacrylamide gel as described above. The results (Figure 2) showed that both proteins bind to CCT in a saturable manner. The fitted curves in the figure were obtained by assuming a single class of site and fitting for both the association constant and the asymptotic extent of binding. The best-fitting values of the dissociation constant, K_d, for actin and tubulin were 0.92 and 0.83 μM, respectively.

Stoichiometry

The best-fitting asymptotic ratios of target protein in the data of Figure 2 were 2.1 for β-tubulin and 1.8 for β-actin, suggesting that two target proteins may bind to each CCT particle. To investigate further the stoichiometry of binding of target proteins to CCT, labeled β-actin or β-tubulin was added to CCT, and CCT−target protein binary complexes were isolated by native gel electrophoresis and analyzed on SDS gels followed by immunoblotting. Known amounts of

[3] As previously shown by Melki and Cowan (1994), β-actin, α-, β-, and γ-tubulin, actin RPV, cap-binding protein, cyclin B, p21^{ras}, and TCP-1α, which share no sequence homology, bind to CCT when presented one at a time. When CCT is absent, all these target proteins, whether mixed together or separate, aggregate and are entrapped at the top of the nondenaturing gels.

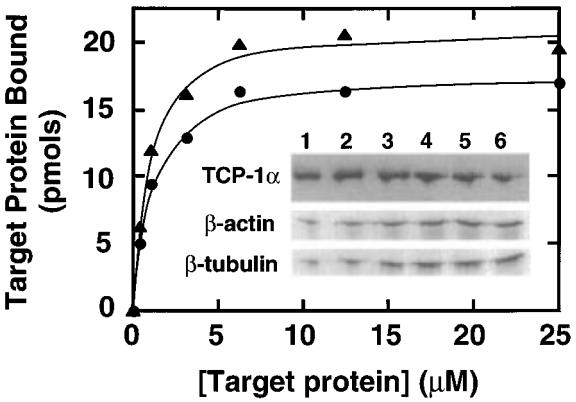

FIGURE 2: Binding of β-tubulin and β-actin by CCT saturation. ^{35}S-labeled target proteins were diluted into folding buffer containing no nucleotide and a constant amount of CCT (10 pmol) and incubated for 30 min at 30 °C prior to analysis of the reaction products on a 4% nondenaturing polyacrylamide gel. The amounts of bound β-actin (●) and β-tubulin (▲) were determined by the use of the phosphorimager. The lines show the results of fitting to the equation $r = ([P]/K_d)/(1 + [P]/K_d)$, where r is the fractional amount bound to CCT, K_d is the dissociation constant, and [P] is the target protein concentration. The amounts of actin and tubulin in the incubation mixtures were 0, 7, 20, 62.5, 125, 250, and 500 pmol. The reaction volume was 20 μL. A Western blot showing the intensity of TCP-1α in each reaction mixture is also shown to indicate its presence in constant amount.

CCT and target proteins were also electrophoresed in the same SDS gel to serve as standards from which to judge the amounts of the unknowns. The ratios of the amounts of bound target proteins to the amount of CCT were then determined by comparison with the standards. Figure 3 shows the results of this SDS gel electrophoresis and immunoblotting. Incubations of increasing amounts of target protein with a constant amount of CCT appear on the left. The five bands characteristic of CCT, but not the target protein, are visible in the Ponceau-Red stained view in Figure 3A. The amounts of CCT present in the complexes were quantitated by immunoblotting (Figure 3B), making use of one of its polypeptides, TCP-1α, as an indicator. The amounts of bound [^{35}S]-β-tubulin and [^{35}S]-β-actin were quantitated (Figure 3C) by use of the phosphorimager. Integration of the intensities of the bands in this typical experiment (panel C, right to left), gave the following stoichiometries for tubulin (0.92, 1.2, 1.55, and 2.0) and for actin (1.42, 1.86, 2.0, and 2.0). Interpolation between standards to obtain the quantities of target proteins (actin and tubulin) bound at saturation is shown in Figure 3D. In accord with the results of Figure 2, saturation of CCT at 0.49 μM (9.5−10.6 pmol) was reached at concentrations of actin or tubulin above 1.3−1.6 μM (30−50 pmol). Table 1 summarizes the data from 16 determinations like that in Figure 3. The data indicate that the two potential binding sites can be occupied at the same time, at least *in vitro* and in the absence of ATP and ADP.

Conformational Changes

Electron Microscopy. Like its prokaryotic homologs GroEL and the thermosome, CCT can adopt two conformational states: one formed when ADP is bound, and another when ATP is bound. These two forms present different views in negative stain, visible in Figure 4. The population of particles is uniform in the presence of ADP (Figure 4A) and resembles rings in the electron microscope. In the

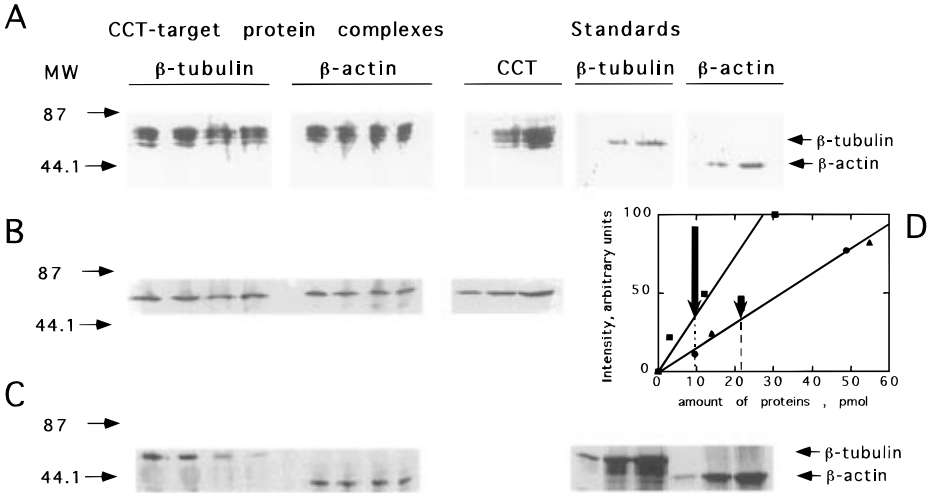

FIGURE 3: Binding of β-tubulin and β-actin by CCT stoichiometry. Stoichiometry of binding was estimated by comparison of amounts of bound polypeptides observed on gels and immunoblots to standards and immunoblots prepared with known quantities of the same polypeptides. (A) Immunoblot stained with Ponceau red prior to probe. (B) The same immunoblot probed with anti-TCP-1α antibody and detected by the ECL technique. The amounts of CCT present in the standard lanes were 3, 12, and 30 pmol. The lanes loaded with target protein−CCT complexes (β-tubulin and β-actin) contained a constant amount of CCT (9.8 pmol) with varying amounts of labeled denatured β-actin (27.3, 69, 138, and 550 pmol) or β-tubulin (32, 80, 160, and 642 pmol). The reaction volume was 20 μL. (C) Phosphorimager detection of target proteins. The amounts of β-actin present in the standard lanes were 9.5, 49, and 131 pmol and those of β-tubulin 14, 55, and 139 pmol. (D) Graphical representation of the intensities of CCT, β-actin, and β-tubulin in the standards as a function of the amount of proteins loaded on the SDS−PAGE. The long arrow marks the position of CCT, and the short arrow marks the coincident positions of actin or tubulin. (■, CCT standards; ●, actin standards; ▲, tubulin standards).

Table 1: Stoichiometry of Target Protein Binding to CCT[a]

CCT (pmol)	actin (pmol)	tubulin (pmol)	ratio
10.1	22.4	0	2.21
11.1	24.8	0	2.23
9.7	20.7	0	2.13
9.5	20.35	0	2.14
6.9	12.5	0	1.81
6.1	11.9	0	1.95
5.3	10.5	0	1.98
7.6	15.4	0	2.02
10.3	0	22.6	2.19
13.8	0	26.9	1.95
13.4	0	27.2	2.03
13.1	0	25.3	1.93
12.9	0	24.8	1.92
11.8	0	24.8	2.10
8.9	0	17.9	2.01
9.3	0	20.1	2.16

[a] Results of determinations of the ratio of bound target protein (β-actin or β-tubulin) to CCT, by the native-gel plus SDS−PAGE method described in the Experimental Procedures.

presence of ATP, a second profile of the CCT particle is obtained (Figure 4F), shaped like a barrel. The ATP preparation, however, is not uniform. A substantial fraction (80%) of the CCT particles (Figure 4B) retain the appearance of the ADP-bound conformation, even in the presence of a large excess of ATP. The cause of this heterogeneity may be either that some of the particles have failed to exchange their nucleotide or that ongoing nucleotide hydrolysis (Melki & Cowan, 1994; Melki *et al*., 1996) causes a fraction of the particles, at any instant, to have ADP bound to them. To distinguish between these two possibilities, we employed AlF_4^-, a structural analog of P_i (Bigay *et al*., 1985; Carlier *et al*., 1988; Combeau & Carlier, 1989), which, when bound together with ADP to nucleotide-binding proteins, mimics the ADP−P_i transition state and blocks further nucleotide exchange (Combeau & Carlier, 1988; Carlier *et al*., 1989; Mittal *et al*., 1996). Figure 4, panels C−E, shows that addition of AlF_4^- to CCT in an ATP-containing solution results in the gradual transformation of these ADP-conformation particles to the ATP-bound conformation. As Figure 4E shows, by 90 min, more than 95% of the particles are found in this conformation. The time required for 50% conversion is about 10 min. The gradual accumulation that we observe must be caused by replacement of ATP and ADP by ADP−AlF_4^-, which mimics ATP but cannot be hydrolyzed. We conclude from these observations that one can generate homogeneous populations of CCT particles in both the ADP and ATP (*i.e*., ADP−P_i) conformations.

Fluorescence Measurements. Figure 5A provides, by measurement of intrinsic fluorescence, an independent indicator of the conformational difference between the ATP- and ADP-bound forms of CCT. The intensity of the fluorescence is 25% greater when ATP is substituted for ADP, without a detectable shift in the wavelength of the emission maximum. This change is consistent with either a greater exposure of tryptophan residues to the aqueous milieu or to a higher degree of liberty of these residues in the ATP-bound form. In Figure 5B, the variation of the fluorescence intensity at the emission maximum (336 nm) is shown as a function of the concentration of added nucleotide. These titrations could be well fitted on the simplifying assumption that each nucleotide binds with a single association constant, yielding values of 2.6×10^4 M^{-1} for ATP and 4.0×10^4 M^{-1} for ADP. The fact that the two titration curves have the same starting point indicates that the original CCT particle, as it emerges from the Superose 6 column, is probably nucleotide-free. The fact that the fluorescence in the presence of saturating amounts of ADP differs from that in saturating ATP shows that the difference between the fluorescence intensities is not due solely to differential affinity. When ATP and AlF_4^- [5 mM NaF and 100 μM $Al(NO_3)_3$] were added to a solution containing CCT in its ADP-bound form (0.025 μM), the fluorescence intensity increased slowly, with a half-time of about 2.4 min at an

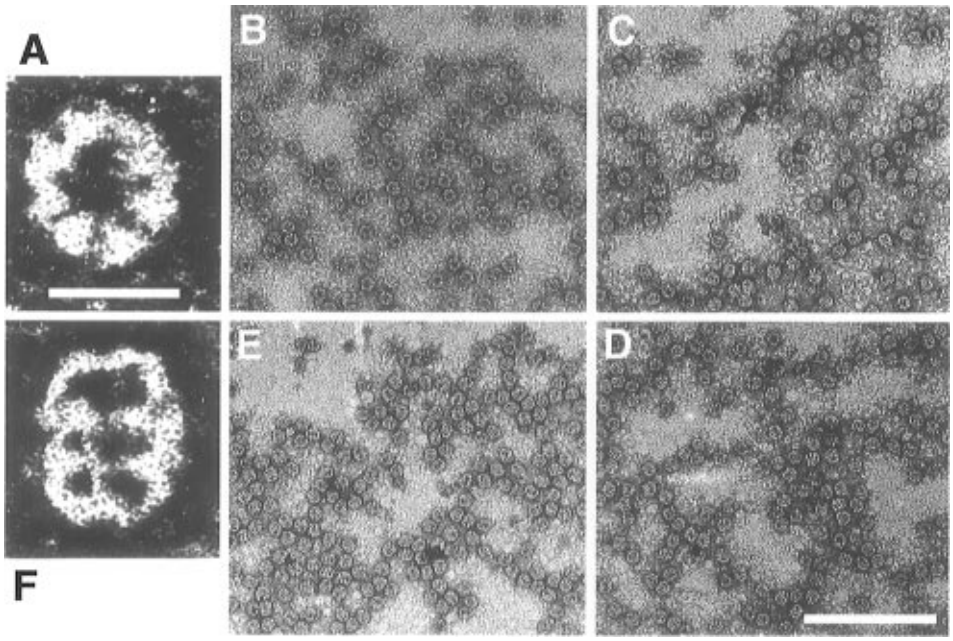

FIGURE 4: Conformations of CCT in the presence of ATP, ADP, and ADP−AlF_4^-. Electron micrograph of negatively stained CCT: (A) in the presence of 100 μM ADP; (F) in the presence of 100 μM ATP. (B−E) Kinetics of accumulation of the ADP-AlF_4^- form of CCT during incubation of CCT in the presence of 100 μM ATP and 100 μM $Al(NO_3)_3$ and 5 mM NaF. Times between nucleotide addition and grid preparation were 2, 30, 45, and 90 min in B−E, respectively. The proportions of the ADP-bound form of CCT in panels B−E are 88% (n = 90), 13% (n = 90), 6% (n = 135), and 1% (n = 100), respectively. Bar = 15 nm in panels A and F and 150 nm in panels B−E.

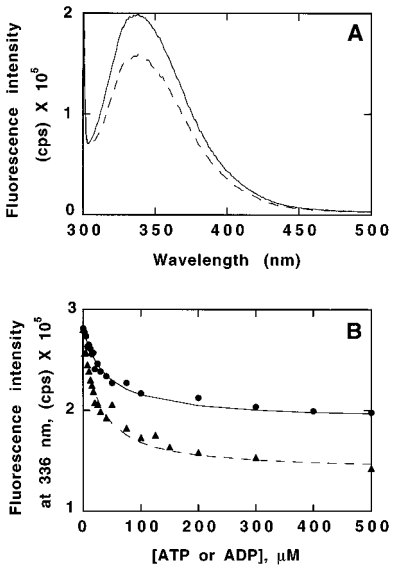

FIGURE 5: Fluorescence emission spectra of CCT in the presence of ATP and ADP. (A) Tryptophan residues were excited at 295 nm, and the emission spectra were recorded from 300 to 500 nm in a 0.2 cm path (slits = 0.7 mm for excitation and 1.5 mm for emission). The CCT concentration was 0.40 μM and the nucleotide concentration was 100 μM in each case, sufficient to saturate the chaperonin's binding sites (Rommelaere *et al*., 1993; Kubota *et al*., 1994). Presence of ATP (solid line), presence of ADP (dashed line). (B) Evolution of CCT tryptophan fluorescence at 336 nm as a function of ADP or ATP concentration. The best fit of the data to a single dissociation constant is shown by the lines (ATP, ● and solid line; ADP, ▲ and dashed line).

ATP concentration of 50 μM and 1.2 min at an ATP concentration of 100 μM.

Sedimentation Velocity. In order to obtain additional insight into the conformational change of CCT, we carried out sedimentation velocity experiments and analyzed them to yield the apparent distribution of sedimentation coefficients, $g^*(s)$. Figure 6A shows typical sedimentation boundaries at a series of equally spaced times. A fast-sedimenting component (arrow) is seen emerging from the mixture, leaving behind a small amount of more slowly sedimenting material. Figure 6B shows the distributions of sedimentation coefficients obtained from experiments with each of the three forms of CCT, *i.e*., ADP−CCT, ADP−AlF_4^-−CCT, and CCT−β-tubulin complex. The distributions are broad, with contributions from molecular species ranging from 5*s* to 50*s*. The material with sedimentation coefficients below the minima at ∼17*s* to ∼19*s* must correspond to dissociated CCT subunits and small amounts (less than 5% of the total amount of proteins) of contaminating proteins, including Hsp70 (Benaroudj *et al*., 1995). To determine whether the slowly sedimenting material corresponds to dissociated CCT particles, CCT (0.1 μM) in the presence of either ADP or ATP (500 μM) was sedimented at 400000*g*, 20 °C for 1 h and the amount of CCT in the supernatant was measured as TCP-1α by Western blot (data not shown). Of the total amount of TCP-1α, 65% was found in the supernatant in the presence of ATP; this proportion was 35% in the presence of ADP. The difference, 30%, must be due to increased dissociation of CCT particles in the presence of ATP. In all cases, however, the prominent maximum corresponding to the fast-sedimenting boundary is evident, and this peak (ranging from 22 to 29 *s*) must correspond to intact CCT particles. From the dimensions reported by Marco *et al*. (1994), and assuming a molecular mass of 800 000 and a partial specific volume of 0.74 cm^3 g^{-1}, one may estimate a sedimentation coefficient of 24*s*, in agreement with this assignment. The fact that the observed and calculated sedimentation coefficients nearly coincide also confirms that CCT particles behave as independent entities, rather than as oligomers, in solution. In the absence of target protein, CCT shows a nucleotide-dependent change in sedimentation coefficient. The ADP−CCT shows a peak centered at 25.6*s*, and the ADP−AlF_4^-−CCT sediments more rapidly, with its peak at 26.8*s*. The higher sedimentation

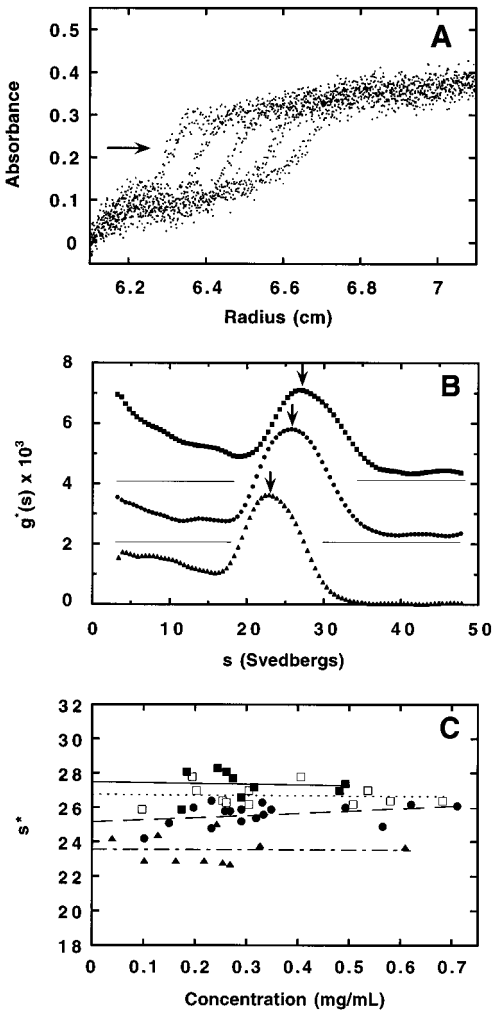

FIGURE 6: Sedimentation behavior of CCT. (A) Typical sedimentation velocity data for CCT. Images of the boundary taken 5 min apart. The steep boundary corresponds to the peak in panel B. (B) Distributions of sedimentation velocity of CCT in the presence of 50 μM ATP and 100 μM $Al(NO_3)_3$ and 5 mM NaF (■), of CCT in 50 μM ADP (●), and of β-tubulin−CCT binary complex (▲). The curves have been displaced vertically for clarity. Arrowheads indicate the positions of the maxima of $g^*(s)$. (C) Sedimentation coefficients of CCT. The values corresponding to the peaks from several experiments are plotted as a function of CCT concentration. CCT in the presence of 50 μM ATP and 100 μM $Al(NO_3)_3$ and 5 mM NaF (■), CCT in the presence of 50 μM ATP (□), CCT in the presence of 50 μM ADP (●), and β-tubulin−CCT binary complex (▲). Rotor speed = 40 000 rpm; temperature 20 °C.

coefficient of the ADP−AlF_4^-−CCT can easily correspond to the "barrel-shaped" particles observed in the electron microscope in the presence of ATP or its ADP−AlF_4^- structural analog. The binary complex, however, shows a lower sedimentation coefficient, 23.5*s*, which is a striking result in view of the fact that it is expected to have a higher molecular mass than vacant CCT (see below).

The concentration dependence of the $g^*(s)$ peaks is shown in Figure 6C. The differences in sedimentation behavior are confirmed, and a linear extrapolation to zero concentration yields sedimentation coefficients of 27.5*s*, 25.2*s*, and 23.5*s* for the ADP−AlF_4^-−CCT, ADP-bound CCT, and binary complex, respectively. The extent of variation of s with concentration over this range is small, leading to the conclusion that the particles are not undergoing major changes in association state. The data obtained at low CCT concentrations in the presence of 50−100 μM ATP without

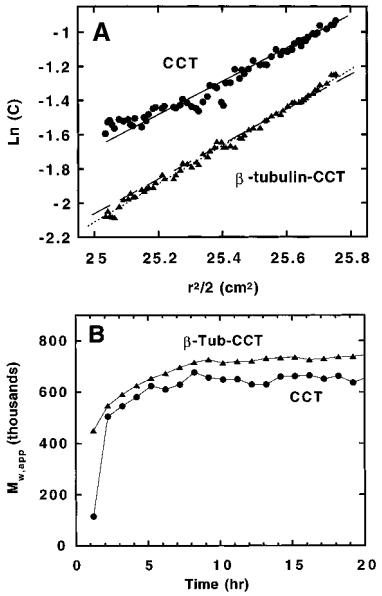

FIGURE 7: Sedimentation equilibrium of CCT and of the CCT−β-tubulin complex. (A) natural logarithm of absorbance vs $r^2/2$. CCT alone (●); isolated complex of β-tubulin and CCT (▲). The overall weight−average molecular weight of each sample was estimated from the slope of the fitted line. The two samples were run simultaneously, to reduce possible systematic errors in this comparison. The solid line shows the best fit of a straight line to the data for CCT alone. The dashed and dotted lines show, respectively, the slopes corresponding to CCT with one β-tubulin bound and with two β-tubulins bound. The best fit, corresponding to the molecular masses reported in Results, is obtained with two polypeptides bound. (B) Time dependence of the overall weight−average molecular masses of ADP−CCT (●), and binary complex (▲).

AlF_4^- are indistinguishable from those obtained in the presence of ATP and AlF_4^-. At higher concentrations, CCT would be expected to hydrolyze ATP quickly, causing the accumulation of ADP-bound CCT. The lower values of the sedimentation coefficient of CCT under these conditions (as distinct from ADP−AlF_4^-−CCT) must reflect this effect. We conclude from these observations that ATP− and ADP−AlF_4^-−CCT have closely similar hydrodynamic properties, distinct from those of ADP−CCT and the CCT−β-tubulin complex.

Sedimentation Equilibrium. In order to examine the molecular state of CCT in solution (*e.g.*, whether monomer or oligomer) and to measure the difference in molecular mass produced by binding of β-tubulin, CCT alone and the CCT−β-tubulin complex isolated by gel filtration were subjected to equilibrium sedimentation at 4 °C in folding buffer containing 50 μM ADP. Figure 7A shows the variation of the logarithm of concentration with (radius^2/2) observed for each sample. The weight−average molecular mass is proportional to the slope of this curve. The CCT−β-tubulin complex has slightly greater apparent molecular mass than CCT alone. The approach to equilibrium is displayed in Figure 7B, which shows the difference in molecular mass to be consistent over time. The molecular mass of the CCT−β-tubulin complex was found to be 739 000 and that of CCT to be 647 000. Although the data presented in Figures 2 and 3 are more sensitive to stoichiometry, the difference in molecular mass, 92 000 ± 30 000 Da, is entirely consistent with the presence of two target protein chains per CCT particle.

DISCUSSION

Target Protein Recognition by CCT

Specificity of CCT. The outcome of the experiments conducted with the artificial mixture of proteins, as well as with individual proteins presented as labeled denatured targets, clearly shows that CCT can recognize a large number of proteins *in vitro* and that it binds them with high affinity in the absence of nucleotide. These experiments also show that CCT is selective: it does not recognize all denatured proteins under these conditions. This broad recognition capacity is still present but harder to identify when CCT is used as an "affinity matrix" to select its own targets from a total soluble cellular extract. Here, although numerous other bands of lesser prominence are present, tubulin and actin form overwhelmingly visible bands in the electrophoretic gel of bound polypeptides, "swamping" the view of the other polypeptides. This occurs because actins and tubulins are the most actively synthesized proteins in the cell. Therefore, they are the most visible because both their specific radioactivity *and* their concentration are high, causing their detection to be overwhelmingly favored. The apparent specialization of CCT for actin and tubulin folding therefore resulted from a gross overestimate of their binding in pulse-chase experiments. In the present study, target proteins of equal specific radioactivity were presented to CCT, so that the broad recognition capacity could be clearly seen and affinities readily compared.

Size of Target Protein. CCT appears to accept target polypeptides of molecular mass up to 120 000 (Figure 1, lane 4). Such an upper limit is consistent with the estimated molecular mass of a globular protein of diameter 6.6 nm. This size may reflect the volume of CCT's peptide-binding cavities that can be deduced from the images of Marco *et al*. (1994).

Stoichiometry of Binding. We estimated the capacity of CCT for target proteins in the absence of ATP by two complementary methods. These conditions were chosen to determine an upper limit of the number of target proteins that can be bound by CCT under conditions where folding does not occur. In the first, the saturating load of labeled model target protein (actin or tubulin) was measured by comparison to a scale of known amounts of the same target proteins (Figures 2 and 3). The results are consistent with a stoichiometry of two target polypeptides per CCT particle. The second method, comparison of molecular masses determined by equilibrium sedimentation, in spite of a relatively large uncertainty, also yielded a ratio of bound target protein to CCT near 2. We therefore conclude that the CCT particle *in vitro* can bind a 2-fold molar amount of target protein and that the dissociation constant for tubulin and actin binding to CCT in the absence of nucleotide appears to be 0.8−0.9 μM.

Although no other measurement of stoichiometry of target protein binding has yet been reported for CCT, the bacterial homolog GroEL has been shown to be capable of simultaneously binding two target proteins in its internal cavities in the absence of nucleotide (Braig *et al*., 1993), as well as binding two of the GroES heptameric rings that are required for the folding of many proteins (Azem *et al*., 1994; Schmidt *et al*., 1994; Llorca *et al*., 1994). This comparison leads us to envisage a similar general mechanism of binding and folding for the two chaperonins, in which both cavities may be filled simultaneously. Binding of target proteins to CCT particles might even be cooperative in that binding of the first target protein chain to the chaperonin particle could increase the affinity of the particle for a second target protein.

Conformational Changes of CCT

Electron microscopy has shown that CCT can adopt at least two conformations in solution. The one that is observed in the presence of ADP appears cylindrical (Gao *et al*., 1992; Lewis *et al*., 1992; Frydman *et al*., 1992) and less compact than the form observed in the presence of ATP (Marco *et al*., 1994). As noted by Gao *et al*. (1992), these two different appearances of CCT must result from a preference for different orientations on the electron microscope grid. One can understand these observations by assuming that CCT particles in their ADP and ATP forms are roughly cylindrical. When applied to an electron microscope grid, the ADP form stands on end, while the ATP form appears to rest with its axis approximately parallel to the plane of the substrate (*i.e*., lying on its side). This difference must result from a conformational change that is reflected in the interaction of CCT's surfaces with the carbon film of the grid.

Marco *et al*. (1994) and Waldmann *et al*. (1995) have briefly noted that the chaperonin in the presence of ATP is not uniform: only a fraction of the particles actually adopt the side-view conformation. In view of the results obtained here, this mixed population appears to be due to ongoing ATP hydrolysis. Indeed, when CCT is blocked in its ADP−P_i form by the addition AlF_4^-, "on-end" views of CCT particles slowly accumulate, until about 95% of the particles adopt this conformation. The characteristic time for the conversion seen in the electron microscope (on the order of 10 min) is compatible with the half-times of 1.2−2.4 min measured by fluorescence, if one takes into account the higher CCT concentrations used in the fluorescence experiments. It is also of the same order of magnitude as that estimated for ATP hydrolysis by empty CCT (Melki *et al*., 1996).[4] ATP hydrolysis and subsequent nucleotide exchange are therefore likely to be responsible for the changes in both fluorescence and particle shape.

Sedimentation velocity permits one to observe these conformational changes in solution and in an independent way. Our data show, first, that the sedimentation coefficients of the ATP and ADP forms differ by about 10%. The ADP−AlF_4^- form sediments more rapidly than the ADP form. Providing that the protein subunit composition of the particle does not change, the ADP−AlF_4^- form must be more compact, or of a shape that presents less frictional resistance than the ADP form, or both. Given the greater tendency of CCT particles to dissociate in the presence of ATP, as demonstrated by the amount of free TCP-1 polypeptide chains seen in the supernatant when CCT is pelleted 400000*g*, and confirmed by the greater amount of slowly sedimenting material observed in the analytical ultracentrifuge, one would expect the ATP−CCT form to sediment

[4] The apparent first-order rate constant for hydrolysis of ATP by CCT is 0.83 min^{-1} at 30 °C in the presence of 1 mM ATP, and that for nucleotide exchange is 0.80 min^{-1} (Melki *et al*., 1996). Under the conditions employed in this work (20 °C and 250 μM ATP), these rate constants would be expected to be about 0.1−0.2 min^{-1}, corresponding to half-times in the range 4−7 min.

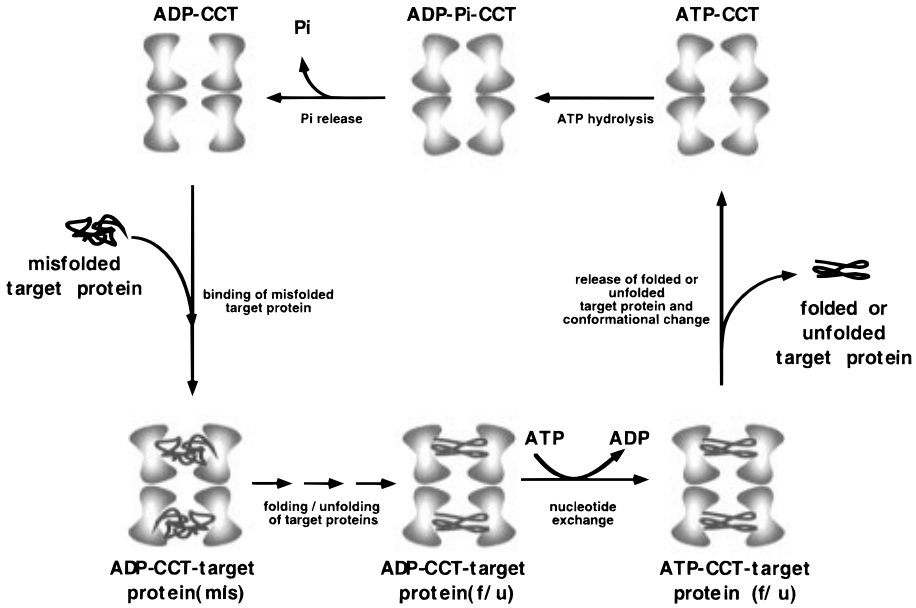

FIGURE 8: Theoretical model for the productive events in chaperonin-assisted folding of target proteins. CCT in its cylindrical ADP-form binds misfolded target proteins strongly (left). Following folding or unfolding of the target protein and nucleotide exchange (bottom), the folded and unfolded target protein is released and CCT adopts a compact "barrel-shaped" form that has a low affinity toward target proteins (right). Following nucleotide hydrolysis, P_i is released in the medium and chaperonin conformation switches to the ADP-bound state that binds strongly misfolded target proteins (top). Final folding of certain target proteins may require several cycles of interaction and release with the chaperonin, with concomitant nucleotide exchange and hydrolysis. Under these circumstances, the folding pathway would correspond to several turns of the cycle of interaction and release of target proteins, with only the last one being productive.

less rapidly if no conformational changes were present. Since the opposite is observed, a conformational change that reduces the hydrodynamic resistance of the ATP−CCT form seems very likely. These observations agree qualitatively with the electron microscopic findings.

Even more striking are the differences of about 10 and 20%, respectively, between the sedimentation coefficient of the tubulin−CCT complex and those of the ADP− and ATP−CCT. In the absence of conformational changes, one would expect the binding of a polypeptide chain to the CCT particle to cause an increase in sedimentation coefficient because of the increased mass. The slight increase in molecular masses observed in sedimentation equilibrium could not by itself cause a *decrease* in the sedimentation coefficient. The observed *decrease* must be due therefore to a conformational change which can be interpreted as an expansion of the particle. In the electron microscope, the binary complex particles resemble the ADP−CCT particles (Marco *et al*., 1994; R. Melki, unpublished observations) in that they appear uniformly circular. Future image reconstruction analysis of CCT−tubulin binary complex particles should reveal the structural details of this conformational change.

The fluorescence results reinforce the conclusion that there is a nucleotide-dependent conformational change in CCT. Furthermore, they provide information about the exposure of tryptophan residues to the aqueous medium. The increase of about 25% in the fluorescence of tryptophan at 336 nm observed in the presence of ATP is consonant with an increase in exposure of tryptophan residues to water (Lakowicz, 1983) and/or the dissociation of a proportion of CCT particles that we observe in the presence of ATP.

Although our data do not extend to the folding reaction itself, they provide considerable information about binding of target proteins to CCT. We have incorporated the current findings into a speculative scheme (Figure 8) to show how they might fit into a functional folding mechanism. The conformational difference produced by the binding of target protein to ADP−CCT (left) and those produced by nucleotide interchange (top) are represented, as well as the fact that CCT can bind two substrate polypeptides at once (bottom). The fact that two target proteins can bind at once to CCT raises the possibility that folding and release may occur at both binding sites. The folding process itself is schematized as a succession of small arrows (folding of target proteins), which are intended to represent either successive cycles of binding and release of the target protein within the protected environment of CCT central cavities (Mayhew *et al*., 1996; Weissman *et al*., 1996; Gray & Fersht, 1993) or conformational changes in CCT's target protein binding domain. These changes lead to the unfolding of the bound misfolded target protein that is released from CCT following nucleotide exchange in a non-native state commited to fold (Todd *et al*., 1994; Weissman *et al*., 1994, 1995).

This model underlines the central role of nucleotide exchange and hydrolysis as the driving force of the conformational changes that occur on CCT. ADP and ATP appear as allosteric effectors between high- and low-affinity conformations of CCT particles, while P_i release acts as a switch mediating the conformational change of the chaperonin and an increase of its affinity toward target proteins, thus completing the cycle. Further identification of the amino acid residues on CCT and target proteins that interact directly with each other, combined with elucidation of the structure and internal motions of CCT, must be achieved in order to gain a full grasp of the mechanism of facilitated folding.

ACKNOWLEDGMENT

We thank Drs. Marie-France Carlier, Dominique Pantaloni, and Serge N. Timasheff for helpful discussions and constant support, and Dr. Patrice Moreau and Robin Leguy for their help in the preparation of the anti-TCP-1α antibody.

REFERENCES

Azem, A., Kessel, M., & Goloubinoff, P. (1994) *Science 265*, 653−656.

Benaroudj, N., Batelier, G., Triniolles, F., & Ladjimi, M. (1995) *Biochemistry 34*, 15282−15290.

Braig, K., Simon, M., Furaya, F., Hainfield, J. F., & Horwich, A. L. (1993) *Proc. Natl. Acad. Sci. U.S.A. 90*, 3978−3982.

Braig, K., Otwinowski, Z., Hedge, R., Boisvert, D. C., Joachimiak A., Horwich, A. L., & Sigler, P. B. (1994) *Nature (London) 371*, 578−586.

Carlier, M. F., Didry, D., Melki, R., Chabre, M., & Pantaloni, D. (1988) *Biochemistry 27*, 3555−3559.

Carlier, M. F., Laurent, V., Santolini, J., Melki, R., Didry, D., Xia, G. X., Hong, Y., Chua, N. H., & Pantaloni, D. (1997) *J. Biol. Chem.* (submitted for publication).

Chen, S., Roseman, A. M., Hunter, A. S., Wood, S. P., Burston, S. G., Ranson, N. A., Clarke, A. R., & Saibil, H. R. (1994) *Nature (London) 371*, 261−264.

Combeau, C., & Carlier, M. F. (1988) *J. Biol. Chem. 263*, 17429−17436.

Combeau, C., & Carlier, M. F. (1989) *J. Biol. Chem. 264*, 19017−19021.

Darnbrough, C., Legon, S., Hunt, T., & Jackson, R. J. (1973) *J. Mol. Biol. 76*, 379−403.

Eisenberg, E., & Moos, C. (1968) *Biochemistry 7*, 1486−1489.

Eisenberg, E., Zobel, C. R., & Moos, C. (1968) *Biochemistry 7*, 3186−3194.

Ellis, R. J., & van der Vies, S. M. (1991) *Annu. Rev. Biochem. 60*, 321−347.

Engel, A., Hayer-Hartl, M. K., Goldie, K. N., Pfeifer, G., Hegerl, R., Müller, S., da Silva, A. C. R., Baumeister, W., & Hartl, F. U. (1995) *Science 269*, 832−836.

Fenton, W. A., Kashi, Y., Furtak, K., & Horwich, A. L. (1994) *Nature (London) 371*, 614−619.

Frydman, J., Nimmesgern, E., Erdjument-Bromage, H., Wall, J. S., Tempst, P., & Hartl, F-U. (1992) *EMBO J. 11*, 4767−4778.

Gao, Y., Thomas, J. O., Chow, R. L., Lee, G.-H., & Cowan, N. J. (1992) *Cell 69*, 1043−1050.

Gao, Y., Vainberg, I. E., Chow, R. L., & Cowan, N. J. (1993) *Mol. Cell. Biol. 13*, 2478−2485.

Gao, Y., Melki, R., Walden, P. D., Lewis, S. A., Ampe, C., Rommelaere, H., Vandekerckhove, J., & Cowan, N. J. (1994) *J. Cell Biol. 125*, 989−996.

Georgopoulos, C. P., Hendrix, R. W., Casjens, S. R., & Kaiser, A. D. (1973) *J. Mol. Biol. 79*, 45−60.

Gething, M.-J., & Sambrook, J. (1992) *Nature (London) 355*, 33−44.

Gray, T. E., & Fersht, A. R. (1993) *J. Mol. Biol. 232*, 1197−1207.

Hartl, F. U. (1994) *Nature (London) 371*, 557−559.

Hartl, F. U. (1996) *Nature (London) 381*, 571−580.

Hartl, F. U., Martin, J., & Neupert, W. (1992) *Annu. Rev. Biophys. Biomol. Struct. 21*, 293−322.

Hemmingsen, S. M., Woolford, C., van der Vies, S. M., Tilly, K., Dennis, D. T., Georgopoulos, C. P., Hendrix, R. W., & Ellis, R. J. (1988) *Nature (London) 333*, 330−334.

Horwich, A. L., Brooks Low, K., Fenton, W. A., Hirshfield, I. N., & Furtak, K. (1993) *Cell 74*, 909−917.

Hynes, G., Sutton, C. W., U, S., & Willison, K. R. (1996) *FASEB J. 10*, 137−147.

Kubota, H., Hynes, G., Carne, A., Ashworth, A., & Willison, K. (1994) *Curr. Biol. 4*, 89−99.

Kubota, H., Hynes, G., & Willison, K. (1995) *Eur. J. Biochem. 230*, 3−16.

Laemli, U. K. (1970) *Nature (London) 227*, 680−685.

Lakowicz, J. R. (1983) *Principles of fluorescence spectroscopy*, Plenum Press, New York.

Langer, T., Pfeifer, G., Martin, J., Baumeister, W., & Hartl, F.-U. (1992) *EMBO J. 11*, 4757−4765.

Lewis, V. A., Hynes, G. M., Zheng, D., Saibil, H., & Willison, K. (1992) *Nature (London) 358*, 249−252.

Lingappa, J. R., Martin, R. L., Wong, M. L., Gamen, D., Welch, W. J., & Lingappa, V. R. (1994) *J. Cell Biol. 125*, 99−111.

Llorca, O., Marco, S., Carrascosa, J. L., & Valpuesta, J. M. (1994) *FEBS Lett. 345*, 181−186.

Marco, S., Carrascosa, J. L., & Valpuesta, J. M. (1994) *Biophys. J. 67*, 364−368.

Mayhew, M., da Silva, A. C. R., Martin, J., Edjument-Bromage, H., Tempst, P. & Hartl, F. U. (1996) *Nature (London) 379*; 420−426.

Melki, R., & Cowan, N. J. (1994) *Mol. Cell. Biol. 14*, 2895−2904.

Melki, R., Vainberg, I. E., Chow, R. L., & Cowan, N. J. (1993) *J. Cell Biol. 122*, 1301−1310.

Melki, R., Rommelaere, H., Leguy, R., Vandekerckhove, J., & Ampe, C. (1996) *Biochemistry 35*, 10422−10435.

Mittal, R., Ahmadian, M. R., Goody, R. S., & Wittinghofer, A. (1996) *Science 273*, 115−117.

Morimoto, R. I., Tissieres, A., & Georgopoulos, C. (1994) in *The biology of heat shock proteins and molecular chaperones* (Morimoto, R. I., Tissieres, A., & Georgopoulos, C., Eds.) pp 1−30, Cold Spring Harbor Laboratory Press, Plainview, NY.

Rommelaere, H., Van Troys, M., Gao, Y., Melki, R., Cowan, N. J., Vandekerckhove, J., & Ampe, C. (1993) *Proc. Natl. Acad. Sci. U.S.A. 90*, 11975−11979.

Roseman, A. M., Chen, S., White, H., Braig, K., & Saibil, H. R. (1996) *Cell 87*, 241−251.

Rothman, J. E. (1989) *Cell 59*, 591−601.

Saibil, H. R., Zheng, D., Roseman, A. M., Hunter, A. S., Watson, G. M. F., Chen, S., auf der Mauer, A., O'Hara, B. P., Wood, S. P., Mann, N. H., Barnett, L. K., & Ellis, R. J. (1993) *Curr. Biol. 3*, 265−273.

Schmidt, M., Rutkat, K., Rachel, R., Pfeifer, G., Jaenicke, R., Viitanen, P., Lorimer, G., & Buchner, J. (1994) *Science 265*, 656−659.

Spiegelman, B. M., Penningroth, S. M., & Kirschner, M. W. (1977) *Cell 12*, 587−600.

Stafford, W. F., III (1992) *Anal. Biochem. 203*, 295−301.

Sternlicht, H., Farr, G. W., Sternlicht, M. L., Driscoll, J. K., Willison, K., & Yaffe, M. B. (1993) *Proc. Natl. Acad. Sci. U.S.A. 90*, 9422−9426.

Studier, F. W., Rosenberg, A. H., Dunn, J. J., & Dudendorff, J. W. (1990) *Methods Enzymol. 185*, 60−89.

Todd, M. J., Viitanen, P. V., and Lorimer, G. H. (1994) *Science 265*, 659−666.

Valentin-Ranc, C., Combeau, C., Carlier, M. F., & Pantaloni, D. (1991) *J. Biol. Chem. 266*, 17872−17879.

Viitanen, P. V., Gatenby, A. A., & Lorimer, G. H. (1992) *Protein Sci. 1*, 363−369.

Waldmann, T., Nimmesgern, E., Nitch, M., Peters, J., Pfeifer, G., Müeller, S., Kellermann, J., Engel, A., Hartl, F. U., & Baumeister, W. (1995) *Eur. J. Biochem. 227*, 848−856.

Weissman, J. S., Kashi, Y., Fenton, W. A., & Horwich, A. L. (1994) *Cell 78*, 693−702.

Weissman, J. S., Hohl, C. M., Kovalenko, O., Kashi, Y., Chen, S., Braig, K., Saibil, H. R., Fenton, W. A., & Horwich, A. L. (1995) *Cell 83*, 577−587.

Weissman, J. S., Rye, H. S., Fenton, W. A., Beechem, J. M., & Horwich, A. L. (1996) *Cell 84*, 481−490.

Willison, K. R., Dudley, K., & Potter, J. (1986) *Cell 44*, 727−738.

Yaffe, M. B., Farr, G. W., Miklos, D., Horwich, A. L., Sternlicht, M. L., & Sternlicht, H. (1992) *Nature 358*, 245−248.

BI962830O